39th Plasmadynamics and Lasers Conference<BR>
23 - 26 June 2008, Seattle, Washington

AIAA 2008-4212

# An Optical Propagation Improvement System and the Importance of Aeroacoustics

A.B. Cain[*], T.T. Ng[†]
Innovative Technology Applications Company, LLC
Chesterfield, MO 63006

E.J. Jumper[‡], D.J. Wittich[§], D. Cavalieri[**]
University of Notre Dame
Notre Dame, IN

E.J. Kerschen[††]
University of Arizona
Tucson, AZ

## ABSTRACT

Use of an airborne platform for a directed energy system is currently severely limited by aero-optic aberrations arising from density variations in air flowing over the aircraft; the primary limitation is for aft pointing applications. Innovative Technology Applications Company (ITAC), in collaboration with the University of Notre Dame (ND), is working to develop, design, construct and test a turret/adaptive fairing that provides a large field of regard for propagation of a lethal beam from an airborne platform at up to transonic speed. The conceptual design incorporates a fairing that includes a tuned cavity between the aperture and the aft-fairing that excites a resonance mode that robustly regularizes optical aberrations imposed by the shear layer over the entire Mach number range. The cavity will be exposed to the flow only when using the beam in an aft pointing direction. Optical-aberration regularization is the exact requirement for robust feed-forward adaptive-optic correction of a laser propagated through the controlled shear layer. This paper will describe the importance of understanding aeroacoustic behavior to effectively develop aero-optic capability that is based on cavity resonances.

[*] Associate Fellow, President
[†] Vice Presidend and Professor – University of Toledo
[‡] Fellow, Professor
[§] PhD candidate
[**] Research Specialist
[††] Senior Member, Professor

## I. State of aero-optics aberration control

Use of an airborne platform for a directed energy system is currently limited by aero-optic aberrations arising from density variations in air flowing over the aircraft. For aft pointing applications, the two primary aero-optic aberration generating phenomena that limit system effectiveness—and the lethal field of regard, in particular—are the separated shear layer and the shock that occurs in transonic flow (Gilbert 1982, Jumper and Fitzgerald 2001, and Hugo and Jumper 2000). Up to now there has been considerable effort put into understanding the optical aberrations due to laser propagation through fully-subsonic flows, first through fundamental flow fields and then from turrets whose flow fields comprised of many of these fundamental flows (Gordeyev et al. 2004).

For an aerodynamic-aft fairing that is larger than the turret in cross section, the flow over the turret at transonic speeds will still be subsonic. This feature simplifies the problem that needs to be addressed. A typical fully-subsonic flow field around a turret is shown in Fig. 1. The flow field is dominated by the separated shear layer behind the turret as well as a strong "necklace" vortex around the base of the turret. Due to its position relative to the laser beam propagation path, the shear layer is the main source of optical aberrations for back-looking angles and thus has attracted the most study.

Various active and passive controls have been investigated as a means of modifying the shear layer to yield a more favorable optical environment. Most of the controls aim to attenuate or modify the large-scale vortices in the shear layer. While varying degrees of success have been achieved, the controls often require a large control input and/or unrealistic operating frequency especially at high speeds. Another approach is to try to reattach the boundary layer over the optical window (Gordeyev et al. 2005). This approach works reasonable well for relatively small azimuth angles, but is much less effective at large azimuth angles due to the rather large adverse pressure gradient encountered. In a previous study, the present ITAC/Notre Dame team has demonstrated success in improving the beam propagation to look-back angles of $123^{\circ}$ back from the freestream flow direction; however, at larger angles none of the techniques explored in that effort were successful. Furthermore, devices used to modify the shear layer can also introduce disturbances with their own optical aberrations. Finally, the devices often need to be placed at a favorable position relative to the separation, which can potentially be problematic since the position of the optical window is not fixed. Thus the thrust of the present effort is to improve beam propagation in aft directions.

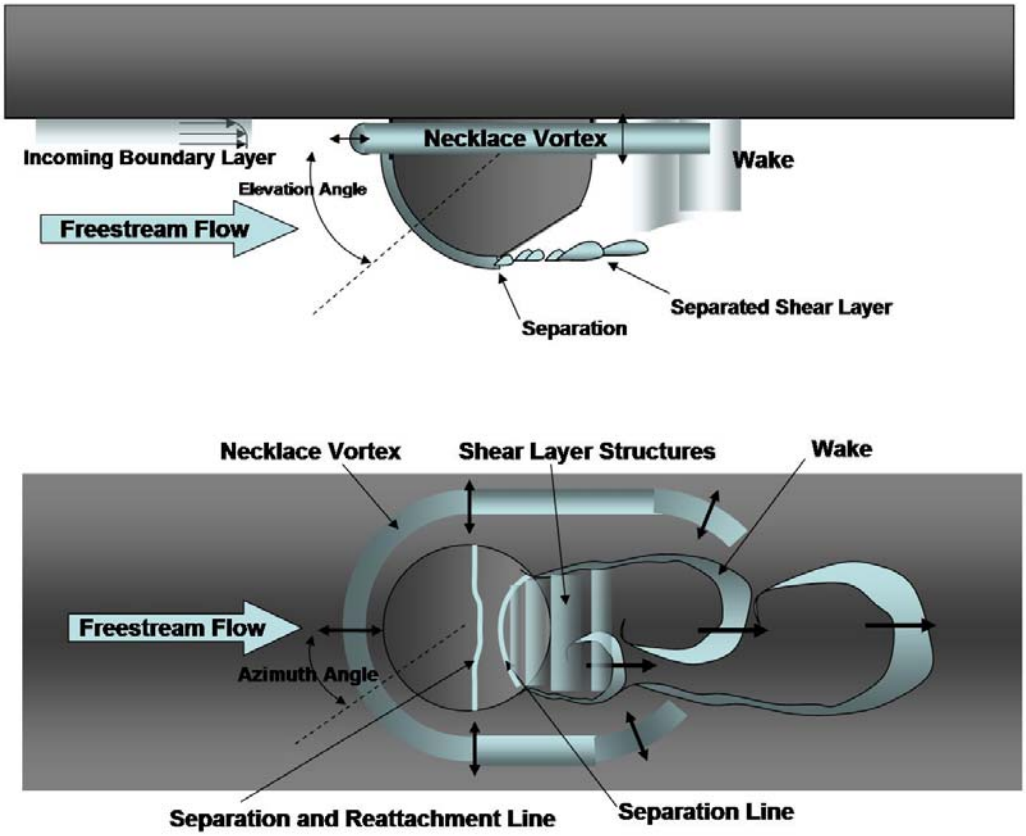


Figure 1 Flow field around a typical turret

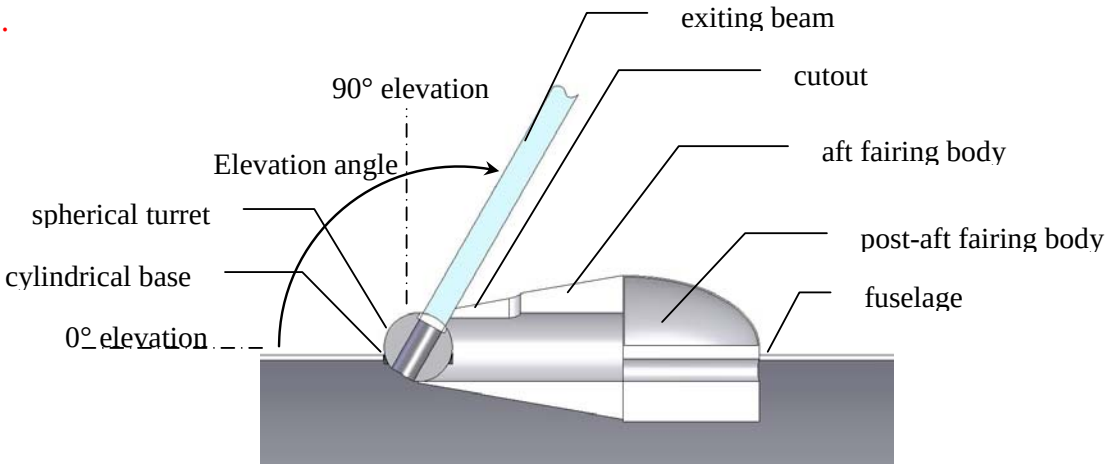


Figure 2a Conceptual side view of possible turret fairing assembly.

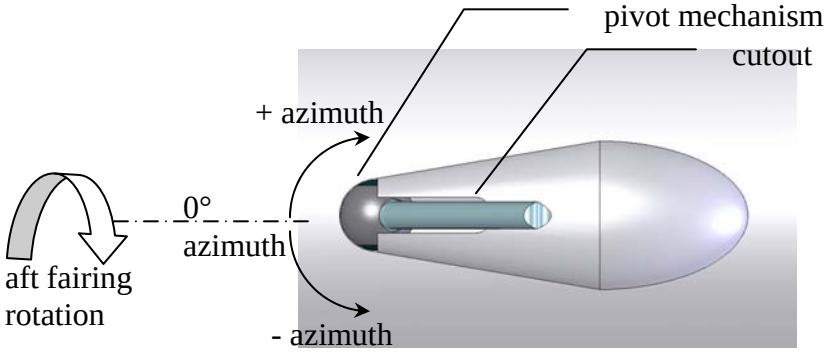


Figure 2b Conceptual top view of possible turret fairing assembly.

In Figures 2a and 2b the proposed solution for improve beam propagation in the aft direction is illustrated. The concept for a possible turret design is also shown. The design consists of a ***spherical turret*** mounted to a ***cylindrical base*** attached to a radially symmetric ***aft-fairing body*** followed by an aerodynamic ***post-aft fairing***. The cylindrical base of the turret contains a ***pivot mechanism*** which allows the sphere to rotate in the elevation direction overall a possible full range of 0°-180°. The cylindrical base itself rotates about its axis of symmetry, i.e. azimuthal angle, over a possible full range of +/-90°. These two degrees of freedom (DOF) provide the ability for the aperture inside the sphere to point the beam, in theory, through a hemispherical volume of space outside of the aircraft. The aerodynamic need for the aft bodies limits this hemispherical field of regard (FOR) to less than that of a true hemisphere. A cutout in the aft fairing body enables the FOR to come close to a full hemisphere. The cutout is homogeneous within

the body of the aft fairing which has the ability to rotate +/-90° about its centerline. Depending on the length of the cutout downstream from the leading edge of its seam to the turret, the beam FOR covers a larger volume and almost approaches that of a full hemisphere in space. The actual shape for the aft portion of the fairing will be more streamlined like that of the ALL. Also, while this conceptual implementation incorporates a cone with a cavity that protrudes below the skin of the aircraft so that it is easy to envision; in fact, the motion of the cavity about the axis shown would probably consist of "leaves" that would come out of a housing at the base of the fairing like an iris or a roll-top, but would store as "folds."

This paper will report on the cavity in a wind tunnel wall data. Some related early work in this area was done by Spee (1966) and Quinn (1963). The theoretical work by Kerschen and Cain (2008), combined with an analysis of experimental data, shows that substantial effects due to wind tunnel confinement can occur in tests with cavities in wind tunnel walls at modest subsonic Mach numbers ($M < 0.75$). The primary issue is the presence of what Kerschen refers to as “nearly-trapped modes.” The presence of nearly-trapped modes results in a modal dominance that greatly exceeds what can be expected in free flight. We believe this behavior occurred in some cases that we studied in experiments conducted at Notre Dame. While this finding was a setback, it enabled the feed-forward demonstration, which has led to the identification of new feed-forward adaptive optic correction techniques now under development.

To address the limitations of the cavity in a wall results, experiments were conducted on a small model of a turret with an aft fairing (with special cavity designs). The experiments suggest a path for successful adaptive optic correction using the feed-forward technique. Unlike the experiments with cavities in the tunnel wall, we believe that the aero-acoustic data from this model is not significantly influenced by the presence of the wind tunnel.

## II. Experimental Setup

All tests were performed in the transonic facilities at Hessert Laboratory for Aerospace Research, University of Notre Dame. The facilities were described in detail in Gordeyev at al. (2005) and interested readers are referred to this reference for a complete discussion. The basic test section is 4” by 4”. The side wall of the test section is instrumented with 8 steady pressure ports to monitor the streamwise evolution of the flow around the cylinder. Ports are positioned 1” apart along a line on the side wall of the test section and 2” from the upper wall. A range of Mach numbers between 0.4 and 0.8 was selected to investigate optical aberrations within a cavity and the shock over a turret model.

Cavities with 4.5-to-1 to 3-to-1 length-to-depth ratios have been designed and constructed for testing in the 4-in.x4-in. transonic tunnel test section. A sketch of a cavity model is shown in Fig. 3. Windows on the top and bottom as well as sides of the test section allow optical access.

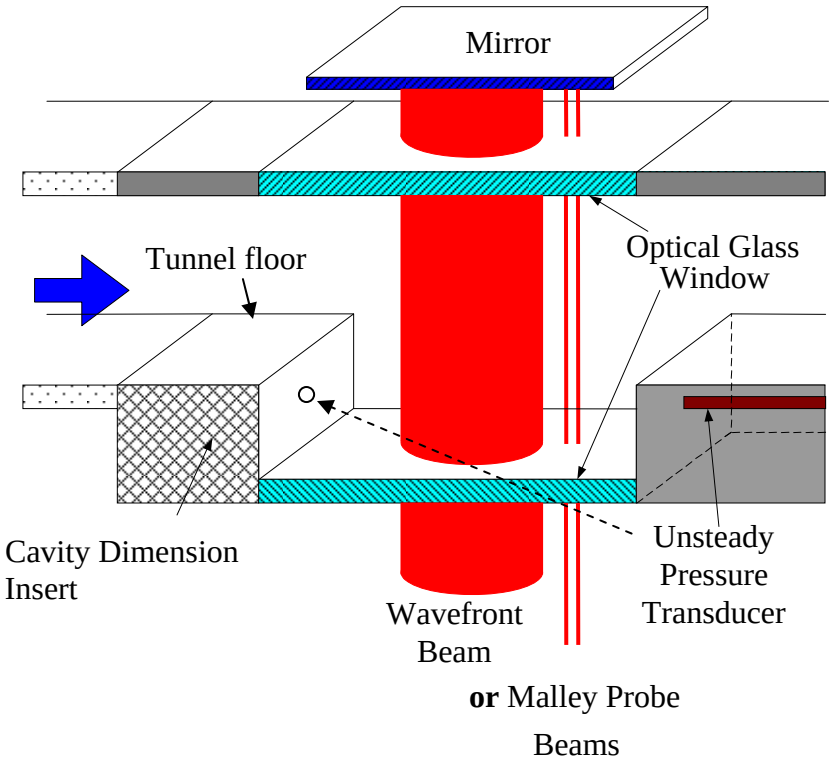


Figure 3 Sketch of the wind tunnel cavity model

In order to measure optical distortions over the cavity two wavefront-measuring instruments were used. The first was a commercially available CLAS-2D 2-dimensional wavefront system. A 2-inch diameter circular laser beam was directed normally through the flat bottom window of the cavity, as shown in Fig. 3. A return mirror outside of the test section was used to co-axially return the laser beam back to the optical bench. The beam thus propagated through the turbulent flow twice, thereby doubling signal-to-noise ratio. Optical distortions were measured using a 2-D Shack-Hartmann wavefront sensor.

A shadowgraph consisting of a frequency-doubling YAG laser and necessary optics was used to visualize the flow. The YAG laser generates 8-ns light pulses at 10 pulses per sec. The short pulse duration allows the capturing of the flow structures in the shear layers as well as the instantaneous position of the oscillating shock downstream of the cavity.

For most of the tests, a Kulite$^{TM}$ pressure sensor placed on the back cavity wall used to monitor the unsteady cavity pressure. Additional pressure sensors were used during the early phase of the study to monitor the pressure upstream of the cavity to detect possible "duct" mode resonance in the test section, and at other positions inside the cavity.

A turret model was designed and constructed for testing in the 4-in.x 4-in. test section. The model, shown in Fig. 4, consists of a 1.5" diameter hemisphere sitting on top of a 0.375" high collar. The model was tested with a fairing as shown in Fig. 4.

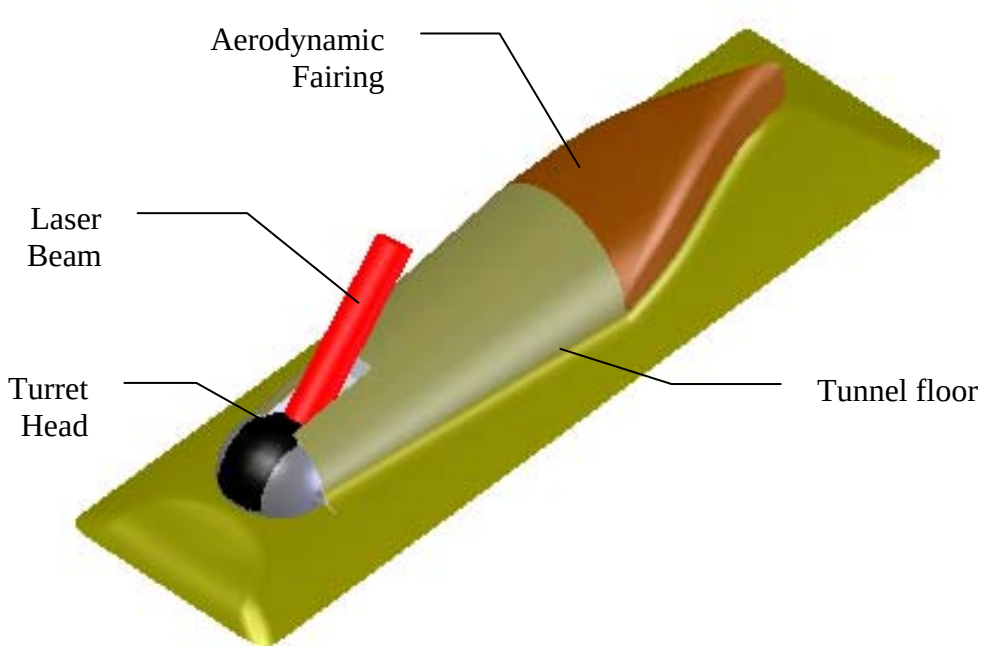


Figure 4 Sketch of the turret model with an aft fairing

## III. Summary of the Aero-optic Results

The original objective in of our work was to simply explore the possibility of using Rossiter excitation to regularize the shear layer over a cavity of reasonable size. A two-dimensional wavefront sensor was used to demonstrate this ability by phase locking the measurement to specific phase angles over a cycle of regularized aberration as it passed over the cavity. This phase locking was accomplished using the signal from a kulite pressure transducer mounted in the forward portion of the cavity. This regularization of the shear layer was also verified by phase-locked shadow graphs as well as analysis of the trigger kulite transducer as well as one at the end if the cavity.

The regularization appeared to be sufficiently robust that we decided to try to perform an actual adaptive-optic correction by feeding forward the regularized dynamic aberration to Notre Dame's Xinetic Deformable Mirror. We were able to perform an adaptive-optic correction of the regularized aberration by phasing up the fed-forward mirror conjugate waveform using the same kulite signal used to phase up the wavefront collections referred to above. This demonstration was far from optimized, and yet the results were both impressive and historic. The correction was achieved for an aberration passage

frequency of ~ 1.1 kHz. Table 1 summarizes the results. The Strehl ratio results in Table 1 give the average Strehl ratio constructed using Fourier Optics from each of 100 wavefront frames at every phase angle and then averaged over every phase angle. In the absence of correction (Uncorrected) the average Strehl ratio is 0.22 with the maximum Strehl ratio of all frames being 0.5 and with the feed-forward conjugate correction (AO Corrected) yielding an average Strehl ratio of 0.61 with the highest Strehl ratio being 0.88. Figures 5a and 5b show a single average frame from the uncorrected case and a single averaged AO corrected frame. As mentioned, this demonstration constitutes the highest-frequency aberration corrected using Adaptive Optics (to our knowledge), breaking the recorded established by Notre Dame for a force Mach 0.78 Shear Layer only a few months earlier, by one and a half times in frequency (i.e., 1.1 kHz vs. 750 Hz).

| | Uncorrected | AO Corrected |
|---|---|---|
| • Mean Strehl Ratio | 0.22 | 0.61 |
| • Max. Strehl Ratio | 0.50 | 0.88 |
| • Power-In-The Bucket | 46% | 77% |
| | (% of Diffraction Limited) | |

**Table 1 Ability to correct for an Aberration using Feed Forward of a Cavity kulite Signal to Drive an Adaptive Optic Cavity (ensemble average)**

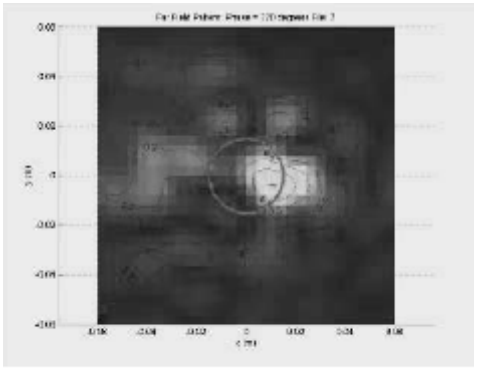

Uncorrected Cavity

Fig. 5a Typical instantaneous frame

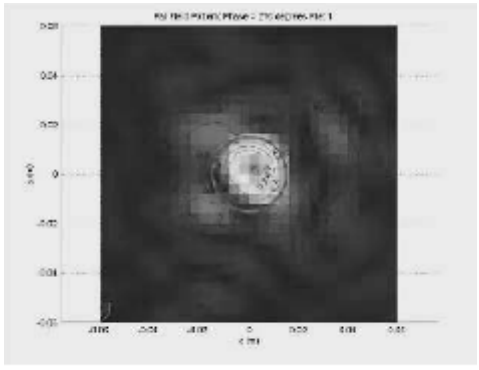

AO Corrected

Fig. 5b Typical instantaneous frame

## III. Background on Aeroacoustic Considerations

A recent theoretical work by Kerschen has introduced the concept of a "nearly-trapped mode". The nearly-trapped mode phenomenon can occur in duct geometries that involve changes in the cross-sectional area, such as for cavity resonance experiments using a cavity-in-wall geometry (see Figure 3). The higher-order cross-stream modes (or

eigenfunctions) play an important role in this phenomenon. Each higher-order mode propagates only for frequencies above its critical frequency. At frequencies below its critical frequency, the mode is cut-off; it decays exponentially with distance along the duct, and transmits no acoustic energy. For the cavity-in-wall geometry, there are two types of modes. First, there are "tunnel modes" in the tunnel regions upstream and downstream of the cavity. Second, there exists "cavity-tunnel modes" in the portion of the tunnel containing the cavity. At modest subsonic Mach numbers, the critical frequency for a higher-order cavity-tunnel mode is smaller than the critical frequency for the corresponding tunnel mode. The region between these two critical frequencies defines the frequency window for the $n^{th}$ higher mode.

When a response is excited in the cavity in the frequency window for the $n^{th}$ higher mode, most of the acoustic energy in the cavity-tunnel mode is trapped in the cavity region; only a small amount of acoustic energy escapes through scattering into lower-order propagating tunnel modes. Since the acoustic radiation is hampered by the $n^{th}$ tunnel mode being cut-off, the energy in the cavity region builds up and the response amplitude greatly exceeds that which could be expected from a similar geometric feature in an external flight environment.

An initial analysis of Kerschen's "nearly-trapped mode" phenomenon was presented in Alvarez and Kerschen (2005). Kerschen and Cain (2008) have since extended the analysis in order to predict the frequency windows where nearly-trapped modes can occur, as a function of Mach number and cavity/tunnel geometry. Other modal properties such as propagation wavenumbers, mode shapes, and the general structure of the modal fields in the cavity-tunnel region have also been determined, in order to elucidate the physics of this phenomenon; see Kerschen and Cain (2008) for details.

## IV. Aeroacoustic Experiments and Subsequent Analysis

Results presented in this section are on experiments that were run on a cavity sits in the floor of the wind tunnel as shown in Fig. 6. The cavity depth (d') is 1.0 inch and the tunnel height (h') is 4.0 inches. Three cavity lengths were studied, (L') of 3.0, 4.0 and 4.5 inches.

Below, we summarize the strongest tones that were found in each case and compare their frequencies to the Rossiter modes. We also include the associated critical frequencies for the appropriate tunnel and cavity-tunnel modes. In all cases we use the two-dimensional modes (i.e. spanwise mode = 0). The critical frequencies for tunnel modes (1,0), (2,0) and (3,0) were computed assuming uniform flow in the tunnel. The critical frequencies for the cavity-tunnel modes were calculated by Kerschen and Cain (2008), Kerschen and Cain assumed that a vortex sheet spans the top of the cavity, that there was no flow within the cavity, and that the flow above the vortex sheet was uniform (see Figure 6).

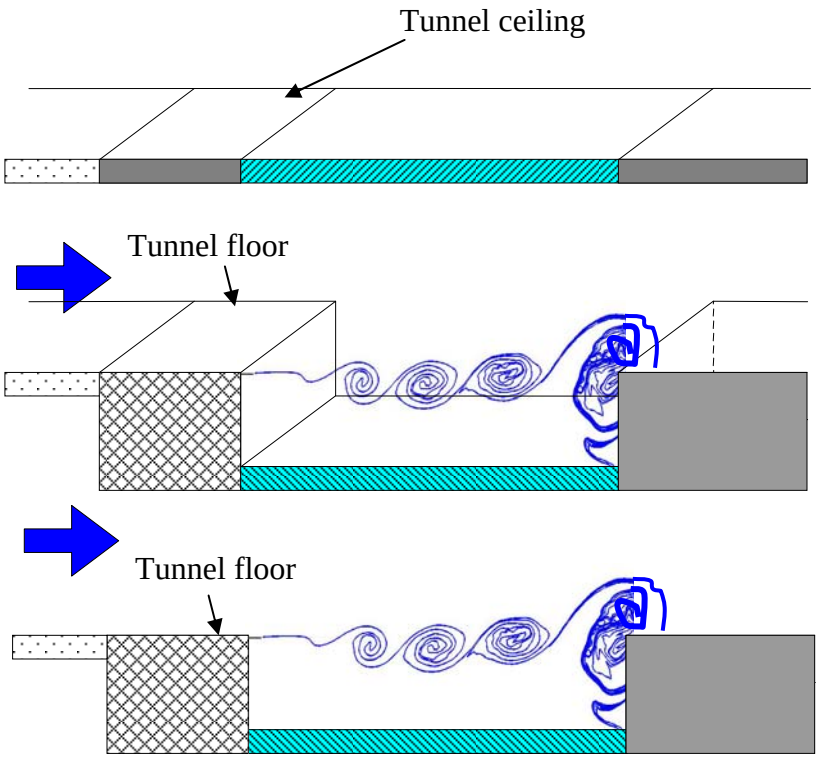


Figure 6 Conceptual image of the wind tunnel-cavity set-up. In the two-dimensional Mathematica analysis the shear layer is approximated by a vortex sheet.

Results in Fig. 7, for the L/D = 3.0 case, show a number of important points. The solid curves with positive slopes are the first 4 Rossiter modes. The 3 solid curves with negative slope are the critical frequencies for the first 3 tunnel modes (recall that these are two-dimensional modes—no spanwise variation). The curves defined by pluses, dashes, and 'X's are the critical frequencies of the first three cavity-tunnel modes. The frequency region between the critical frequencies of the $n^{th}$ "cavity-tunnel mode" and the $n^{th}$ "tunnel mode" is referred to as the "$n^{th}$ frequency window". These windows exist for Mach numbers less than 0.75 when the cavity depth is 25% of the tunnel height. As discussed above, when the experimental peak response frequency is in these regions, it corresponds to a "nearly-trapped mode". Essentially, the cavity shear layer disturbance excites the propagating (and nearly resonant) cavity-tunnel mode (because the frequency is higher than the critical frequency of the $n^{th}$ cavity-tunnel mode), but very little energy propagates away upstream or downstream of the cavity (because the frequency is below the critical frequency of the $n^{th}$ tunnel mode frequency). Note that for the M = 0.625 case there are 3 nearly-trapped mode responses that fall near to the first, second, and third Rossiter modes. Remarkable as it seems, all the Mach number cases examined for the L/D = 3.0 cavity result in nearly-trapped mode responses.

The amplitudes of the dominant frequency responses for the L/D = 3.0 case vary by almost three orders of magnitude. Table 2 provides details of the frequency and amplitude pairs for each Mach number. The relatively large amplitude of the dominant modes is due to the presence of nearly-trapped modes. We expect a free flight cavity to exhibit a very different behavior, because there is no analog for the tunnel walls to interact with the cavity. Thus, cavities in free flight will be free of nearly-trapped modes.

The highest amplitudes for these nearly-trapped mode results for L/D = 3.0 are for the two highest Mach number cases. We believe that the disturbance levels saturate at finite amplitude primarily due to the Kelvin-Helmholtz instability growing the shear layer thickness to the point that the dominant frequency disturbance can no longer extract energy from the mean shear layer profile. In the range of Mach numbers considered here, the shear layer instability saturation levels scale closely with the velocity difference across the shear layer, and the velocity difference across the shear layer scales with Mach number. Therefore, it is not surprising that the highest Mach number cases have the highest amplitude.

Two other factors also contribute to the nearly-trapped mode at the highest Mach number having the highest amplitude for L/D = 3.0. First, the lower Rossiter modes often have higher energy levels than higher Rossiter modes. At the two highest Mach numbers of L/D = 3.0, the reponse is at a frequency very close to the $1^{st}$ Rossiter mode. The response at M = 0.675 is probably enhanced by the close match seen with the frequency of the $1^{st}$ Rossiter mode. Second, the energy trapping is more complete when the response lies in the $1^{st}$ frequency window, since only the plane wave mode is available to propagate energy away in the tunnel for this case. In contrast, other tones seen in Figure 5 lie in the $2^{nd}$ and $3^{rd}$ frequency windows, where additional modes are available to propagate energy away in the tunnel.

Note that the above discussion depends on all the dominant resonant responses being nearly-trapped modes (as was the case for the L/D = 3.0 cavity); if a mix of nearly-trapped and non-trapped modes is present, then these arguments on the scaling cannot be expected to hold (as will be discussed later).

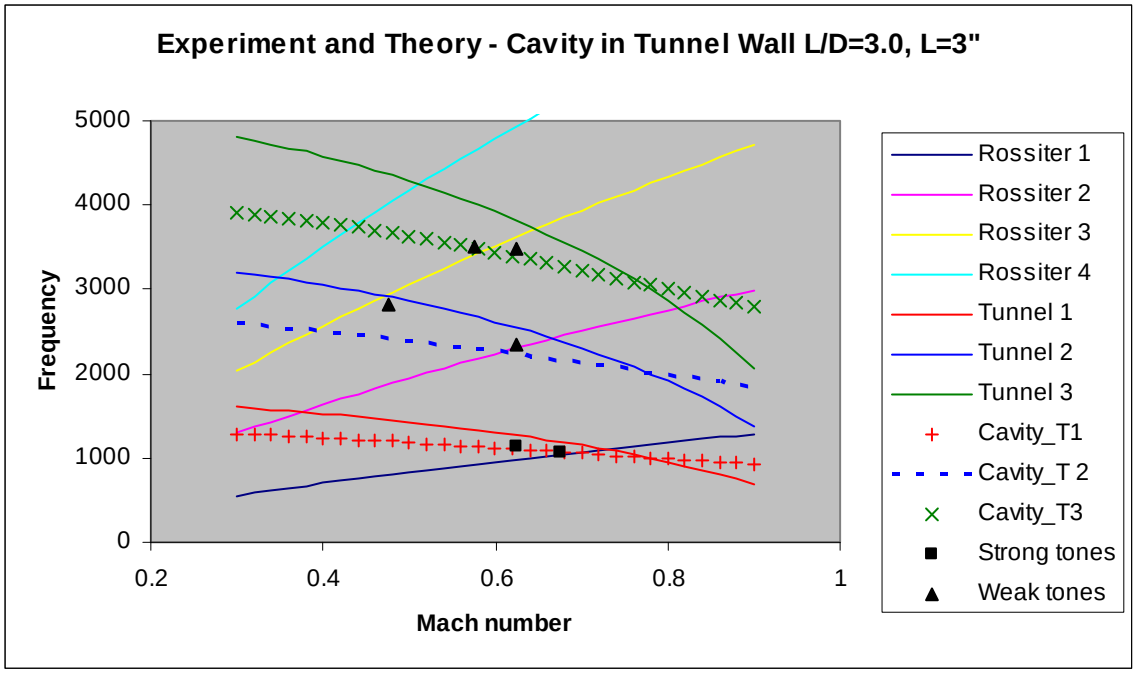


Figure 7 Plot of the first 4 Rossiter modes (continuous lines with positive slope), the first 3 tunnel modes (continuous lines with negative slope), the first 3 cavity-tunnel modes (pluses, dashes, and Xs), and the kulite dominant tones from the upstream wall of the cavity.

L=3.0 Port 5

| Mach | Freq 1 | Amp 1 | Freq 2 | Amp 2 | Freq 3 | Amp 3 |
|---|---|---|---|---|---|---|
| 0.475 | 2830 | 3.92E-05 | | | | |
| 0.575 | 3504 | 5.92E-05 | | | | |
| 0.625 | 1135.5 | 2.44E-03 | 2356.5 | 8.96E-04 | 3491 | 1.49E-04 |
| 0.675 | 1071.5 | 2.64E-02 | | | | |

Table 2 Frequency and amplitude data for L/D=3.0

Figure 7 and Table 3 present theoretical and experimental findings for the L/D = 4.0 cavity. The dominant frequencies at the lowest three Mach numbers all correspond to nearly-trapped modes.

Unlike with the L/D = 3.0 cavity, the highest amplitude response for the L/D = 4.0 cavity is not at the highest Mach number (M = 0.675). However, it is important to note that the tone at the highest Mach number does not lie in a frequency window. Since the tone at M = 0.675 is not in a frequency window, the energy supplied to the active cavity-tunnel mode can be easily radiated away from the cavity by the corresponding tunnel mode. Thus, this case ends up having the lowest amplitude. Hence, the M = 0.675 case clearly illustrates the impact that the cavity/tunnel interactions can have.

The highest amplitudes for the L/D = 4.0 cavity occur at M = 0.525 and 0.575; these are nearly-trapped modes that lie in the 2nd frequency window. This emphasizes the importance of the nearly-trapped mode phenomenon. Regarding the difference in amplitude between the responses at M = 0.525 and 0.575, little significance should be attached to the differences in amplitude for these two cases, since measurements have been made at only two points in the cavity.

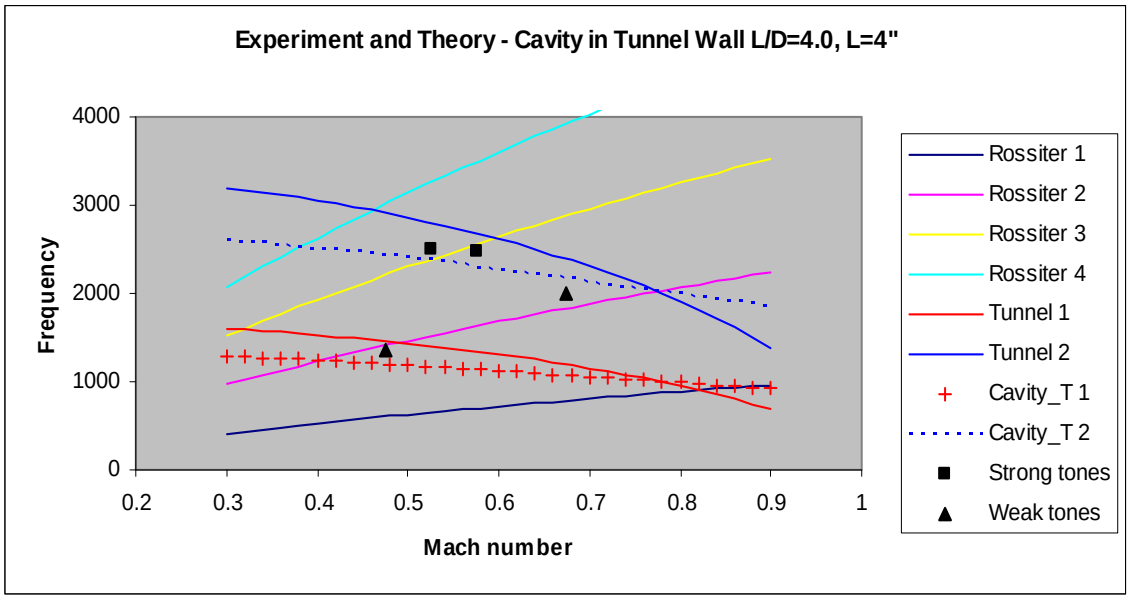


Figure 8 Plot of the first 4 Rossiter modes (continuous lines with positive slope), the first 2 tunnel modes (continuous lines with negative slope), the first 2 cavity-tunnel modes (pluses and dashes), and the kulite dominant tones from the upstream wall of the cavity.

L=4.0 Port 5

| Mach | Freq | Amp |
|---|---|---|
| 0.475 | 1358 | 1.23E-03 |
| 0.525 | 2494 | 1.09E-01 |
| 0.575 | 2469.5 | 6.66E-02 |
| 0.675 | 2006.8 | 1.25E-04 |

Table 3 Frequency and amplitude data for L/D=4.0

Results for the L/D = 4.5 cavity are presented in Figure 7 and Table 4. The most striking feature for this configuration is that the lowest Mach number (M = 0.475) has the highest amplitude response. The amplitude is an order of magnitude higher than the corresponding tone at M=0.475 in Table 3 for the L/D = 4.0 cavity. One possible explanation for this difference is that in the L/D = 4.0 case, the response is very close to the intersection of the 2nd Rossiter mode frequency and the 1st tunnel mode critical frequency. This may enable the L/D = 4.0 cavity to leak energy (at this frequency) faster than for the L/D = 4.5 cavity.

The results for the higher Mach number case (M = 0.675) of the L/D = 4.5 cavity are especially interesting because this case had three spectral peaks, rather than the single peak observed in the other cases. The two lower frequency peaks are not in the frequency windows, and therefore are not nearly-trapped modes. Thus, the energy at these frequencies can propagate away from the cavity quite easily, leading to relatively small resonance amplitudes.

The one nearly-trapped mode that occurs for M=0.675 and L/D=4.5 has the highest amplitude (for this Mach number and L/D), but the amplitude is only slightly higher than that seen in the L/D = 4.0 cavity at this Mach number (which was not a trapped mode response). In contrast, the tone for M=0.675 and L/D = 3.0, which was a trapped mode response, had an amplitude that was higher by two orders of magnitude. There are two factors that may explain the lower response level for the 3453 Hz tone at M = 0.675 and L/D = 4.5. First, the tone at L/D = 4.5 is excited by the 4th Rossiter mode, while the tone at L/D = 3.0 is excited by the 1st Rosstier mode. The higher Rossiter modes typically have less energy than the lower Rossiter modes. Second, the tone for L/D = 4.5 is in the 3rd frequency window, while the tone for L/D = 3.0 is in the 1st frequency window. For the 1st first frequency window, the only propagating mode available to transfer energy away from the cavity region is the plane wave mode in the tunnel. In contrast, for the third frequency window, there are three propagating modes available to transfer energy away from the cavity region, the plane wave mode and the 1st and 2nd tunnel modes. In general, we expect higher amplitudes when the response is in the lower frequency windows.

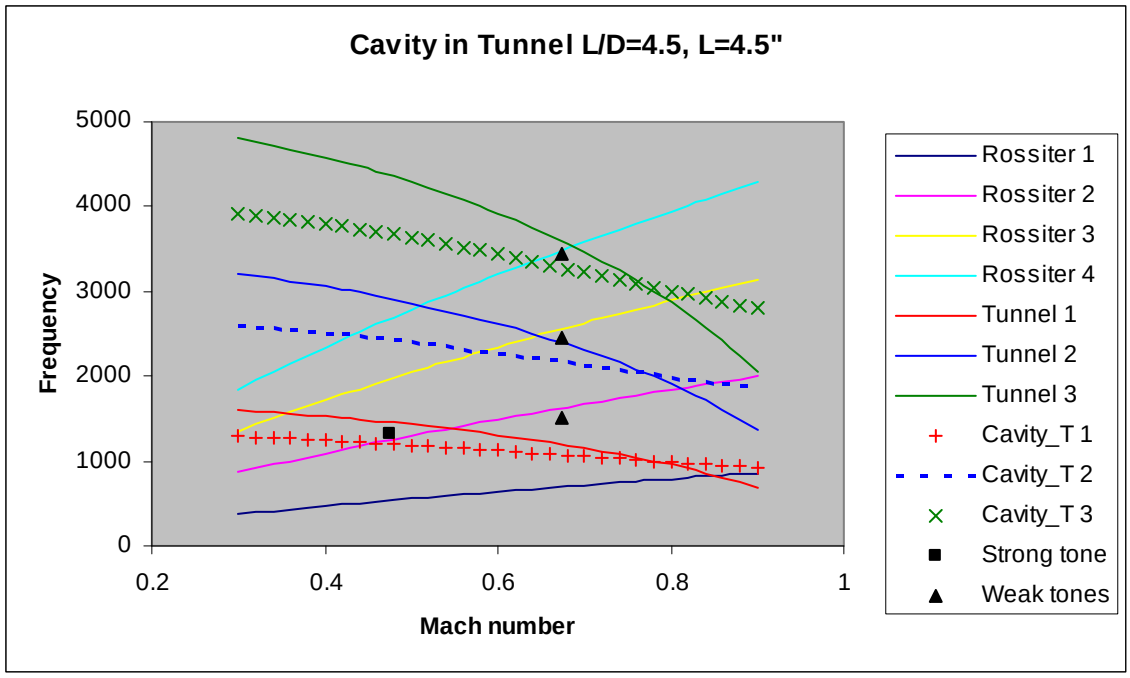


Figure 9 Plot of the first 4 Rossiter modes (continuous lines with positive slope), the first 3 tunnel modes (continuous lines with negative slope), the first 3 cavity-tunnel modes (pluses and dashes), and the kulite dominant tones from the upstream wall of the cavity.

L=4.5 Port 5

| Mach | Freq 1 | Amp 1 | Freq 2 | Amp 2 | Freq 3 | Amp 3 |
|---|---|---|---|---|---|---|
| 0.475 | 1310.8 | 1.28E-02 | | | | |
| 0.675 | 1520 | 5.97E-05 | 2452.4 | 1.40E-04 | 3452.8 | 1.50E-04 |

Table 4 Frequency and amplitude data for L/D=4.5

## V. Conclusions on the Cavity in a Wind Tunnel Wall Experiments

Analysis of kulite data from cavities placed in a wind tunnel wall has shown the importance of aero-acoustics mode interaction considerations. Tunnel modes, cavity-tunnel modes and experimental response data have been analyzed for multiple Mach numbers and L/D ratios. The "nearly-trapped mode" behavior that was identified by Kerschen has been found to significantly influence the results. Amplitude variations in the spectral peaks are shown to vary by up to three orders of magnitude. The data

examined here shows that the aeroacoustic behavior is consistent with Kerschen's conceptual model of this phenomenon. The enhancement of resonance amplitudes is particularly significant when the tone falls in the 1st frequency window. The amplitude of the spectral peaks of a nearly-trapped mode can scale with Mach number, but the matching with generic Rossiter mode energy levels, and the proximity of the Mach number/peak frequency pair to the intersection of a Rossiter mode and tunnel critical frequency (as functions of Mach number), also appear to play a major role. Even if the response is a nearly-trapped mode, it appears that such opportunities for the increased radiation of energy can be a very important factor in determining which Mach number/frequency pair has the highest amplitude.

## VI. Experiments on a Small Turret with an Aft Fairing: a Promising Path to Feed-forward Adaptive Optic Correction

In addition to the experiments discussed above, additional experiments were conducted on a small turret with an aft fairing. While the aft fairing does contain an L/D = 4.0 cavity, the cavity bottom is not recessed into the wall. Hence these experiments may be expected to be unaffected by the nearly-trapped mode phenomenon. Initial experiments were conducted with a "standard cavity" (with no additional fittings). Bolstering the contention that nearly-trapped modes were absent from this experiment, the kulite data showed no strong response tones.

The next experiments were conducted with small covers placed over either the forward, aft, or both portions of the cavity. These partial cover experiments also examined different cover lengths. Figure 10 shows a schematic of the test article with an aft cover. In all, a total of 8 geometries were tested at 4 Mach numbers. Kulite data was collected upstream of the model, behind the hemisphere, and at the downstream end of the cavity (as illustrated in Figure 11).

Figure 12 through Figure 15 are the spectra from the kulites for a configuration with an aft cover over the fairing cavity. These spectra clearly show the presence of strong tones with this design. By optimizing L/D, cover length, and adding an acoustic liner, further control of the tonal response can be obtained--hopefully a single strong tone for a full range of Mach numbers. Such an optimized configuration will enable a successful feed-forward capability without involving nearly-trapped modes.

Figure 16 shows the frequency response as a function of Mach number for the small turret/aft fairing cavity set-up (see Figures 10 and 11). The plot contains a number of reference curves – the first 2 Rossiter modes which may behave differently due to the aft cover. Also plotted are the first 2 vertical tunnel modes and an estimate for the open-closed ¼ wavelength tube response. The open-closed tube response should be expected to be much lower than the basic curve since the length of the opening is not long compared to the tube "diameter". Also included in determining the ¼ wavelength frequency is a length end correction estimated at 0.86 times the tube "diameter". A shorter cover case (L/D=3.0) is presented in Figure 17. One big difference shown in

Figure 17 is that the frequency versus Mach number plots looks as if the responses line up with the tunnel (1,1) mode. At this time we don't have enough information to make conclusive statements though further studies with more kulites will clarify things.

After the apparent success of the basic small model design shown in Fig. 10, versions of the small model with special features were built using stereo lithography techniques (SLA). An extensive testing program continued and examples of the results are shown in Figures 18 and 19. These results are important as they show that it is possible to obtain a nearly constant frequency tonal response over a significant range of Mach numbers. The strong tone can be expected to excite a dominant Kelvin-Helmholtz instability that controls the dominant optical aberration. Thus having a near constant frequency over a range of Mach numbers would minimize the required bandwidth of an adaptive optic to correct the resulting optical aberration.

## VII. Conclusions

Analysis of data from experiments on a cavity in a wind tunnel wall show "near trapped mode" responses that contain far more acoustic resonance energy than a free flight situation would likely have. Follow-on studies of a small turret with an aft fairing containing a cavity should not be able to respond in a near trapped mode behavior. However, one set of experiments on the turret fairing case seems to show excitation of a (1,1) tunnel mode. More kulites will clarify this result. Future work will address optical measurements. Two very important points need to be made regarding the current results. The first point to be made is that strong single resonances set-up with an aft cover on the fairing cavity. The second point is that the small model turret fairing studies show a small variation in the response tone over a range of Mach number. This will produce a limited range of the spatial aberration wavelengths and should ease requirements for a deformable mirror correction. We believe we have identified a very promising geometry for flow control and enabling the adaptive optic correction.

## VIII. Acknowledgment

This work was done under support from an AFRL/RDS SBIR with Drs. Larry Weaver and Frank Eaton serving as the Program Manager. The views presented are those of the authors and not necessarily those of AFRL or the US Government.

## References

J. O. Alvarez and E. J. Kerschen (2005) "Influence of Wind Tunnel Walls on Cavity Acoustic Resonances," AIAA-2005-2804.

K.G. Gilbert, "Overview of Aero-Optics," Aero-Optical Phenomena, Eds. K.G. Gilbert and L.J. Otten, Vol. 80, Progress in Astronautics and Aeronautics, AIAA, New York, 1982, pp. 1-9.

S. Gordeyev, T. Hayden and E. Jumper, " Aero-Optical and Hot-Wire Measurements of the Flow Around the Hemispherical Turret With a Flat Window ", AIAA paper 2004-2450, 2004.

S. Gordeyev, E. J. Jumper, T. T. Ng and A. B. Cain, "The Optical Environment of a Cylindrical Turret with a Flat Window and the Impact of Passive Control Devices", AIAA paper, 2005-4657, Toronto, 2005.

R.J. Hugo, and E.J. Jumper, “Applicability of the Aero-Optic Linking Equation to a Highly Coherent, Transitional Shear Layer,” Applied Optics, 39 (24), August 2000, pp. 4392-4401.

E.J. Jumper, E.J., and E.J. Fitzgerald, “Recent Advances in Aero-Optics,” Progress in Aerospace Sciences, 37, 2001, pp.299-339.

E. J. Kerschen and A.B. Cain, (2008) “Aeroacoustic Mode Trapping for a Wind Tunnel with a Cavity in the Wall,” AIAA-2008-4213, Plasma Dynamics and Lasers Conference in Seattle, June 2008.

Spee,B. M., “Wind tunnel experiments on unsteady cavity flow at high subsonic speeds,” AGARD 1966.

Quinn, B., “Flow in the Orifice of a Resonant Cavity,” AIAA Student Journal 1963.

Wittich, D. J., Duffin, D. A., Jumper, E. J., Ng, T., and Cain, A. B., “Feed-Forward, Adaptive-Optic Correction of a Compressible Shear Layer over a Rectangular Cavity,” Directed Energy Systems Symposium, Monterey, California, Mar 2007.

Wittich, D. J., Jumper, E. J., Cain, A. B., and Kerschen, E. J., “An Acoustically Regularized Shear Layer for Feed-Forward Adaptive-Optic correction,” Directed Energy Systems Symposium, Monterey, California, Mar 2008.

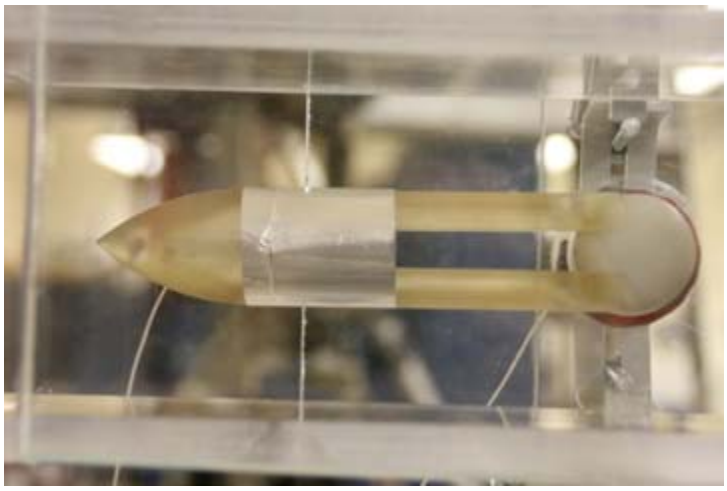

Figure 10 Turret model with a cover over the aft portion of the cavity.

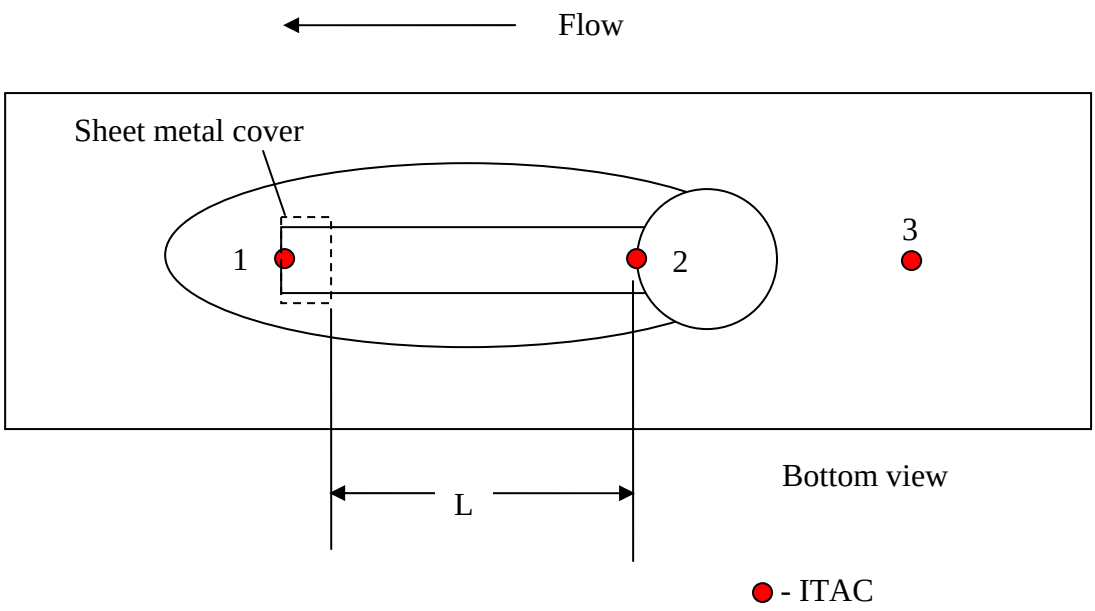


Figure 11 Schematic showing the location of the kulites in the small turret aft fairing experiments.

**Pressure port 1**

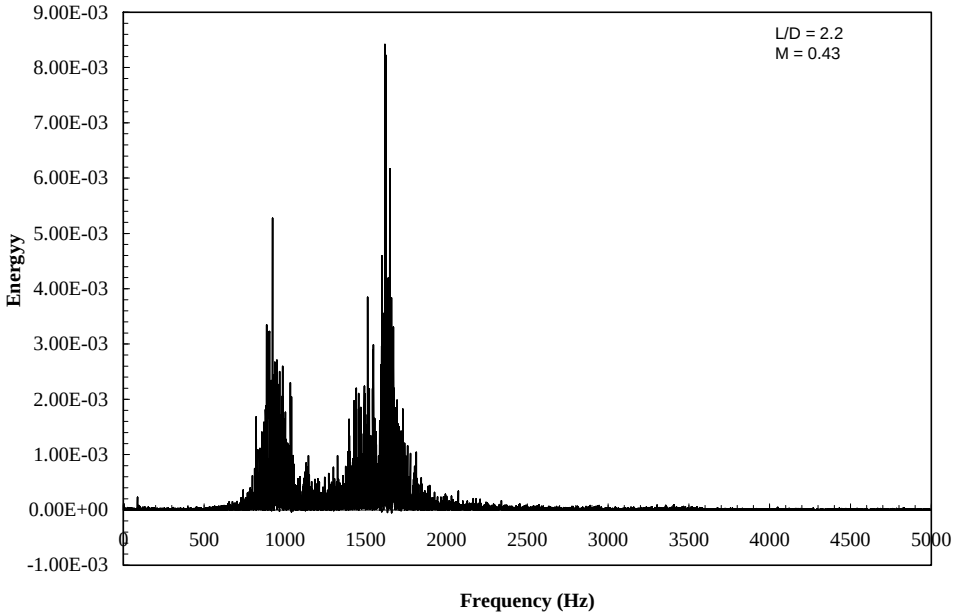


**Pressure port 2**

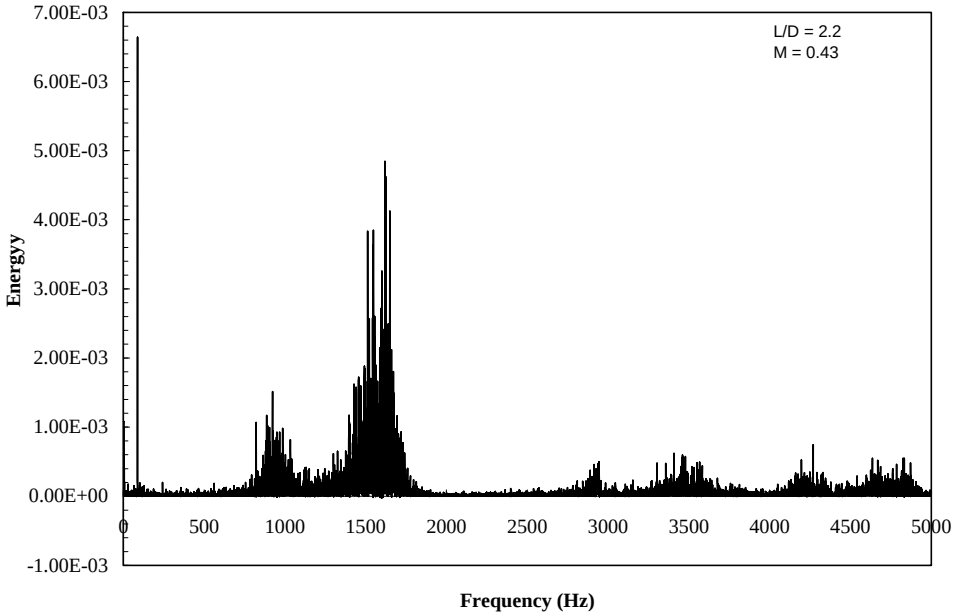

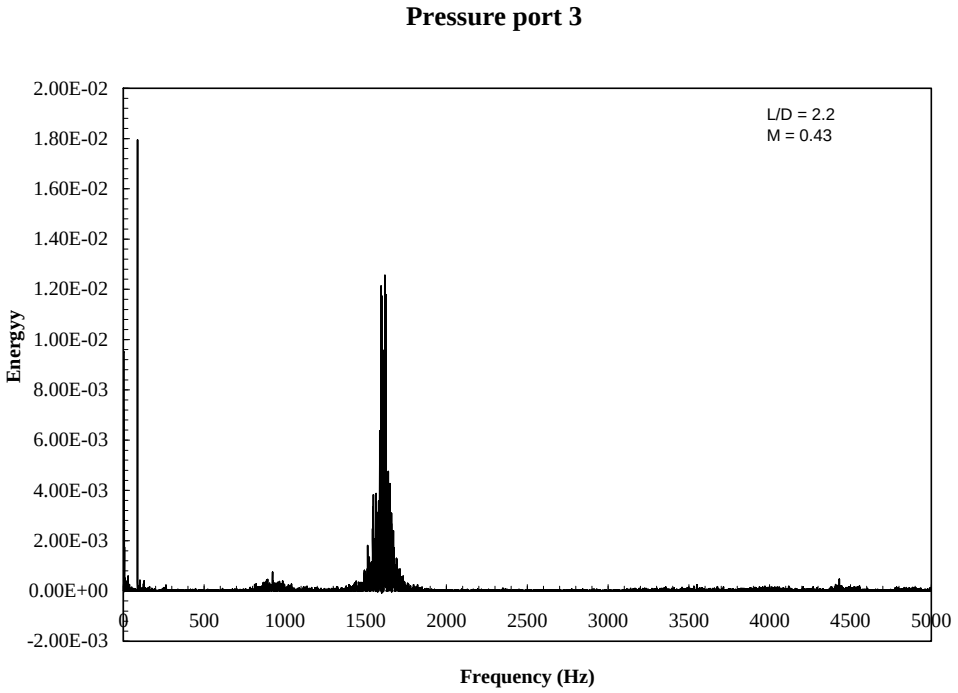


Figure 12 a), b), c) Spectra from kulites at ports 1, 2, and 3 respectively, M=0.43, L/D=4.0 with an aft cover length equal to 0.45 of L.

**Pressure port 1**

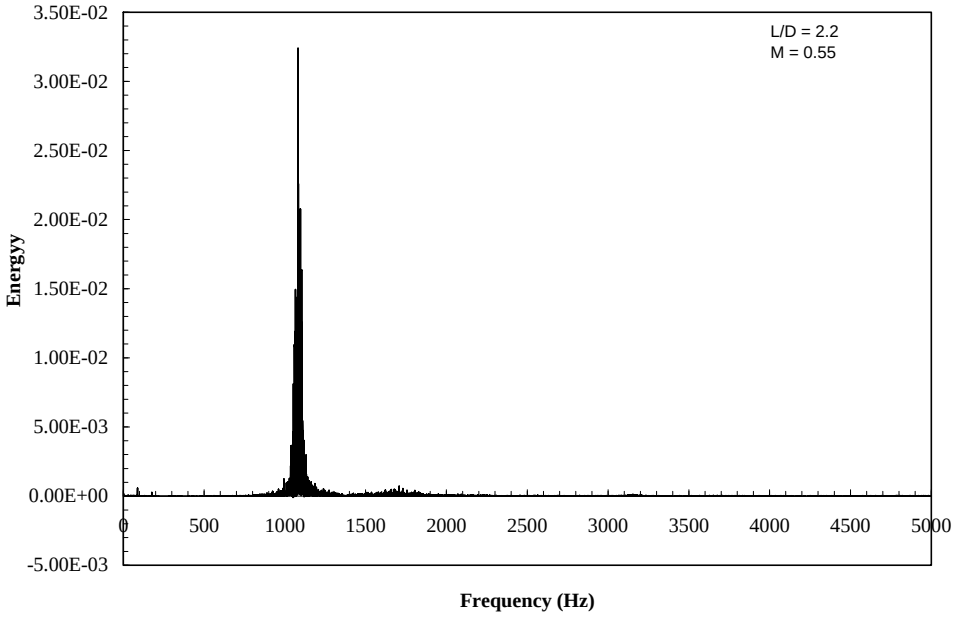


**Pressure port 2**

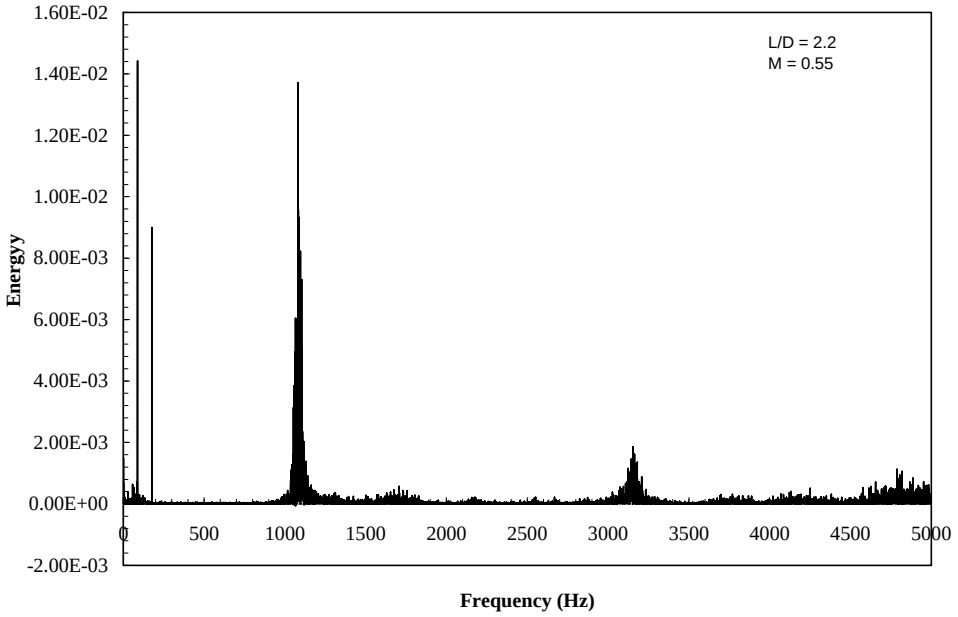

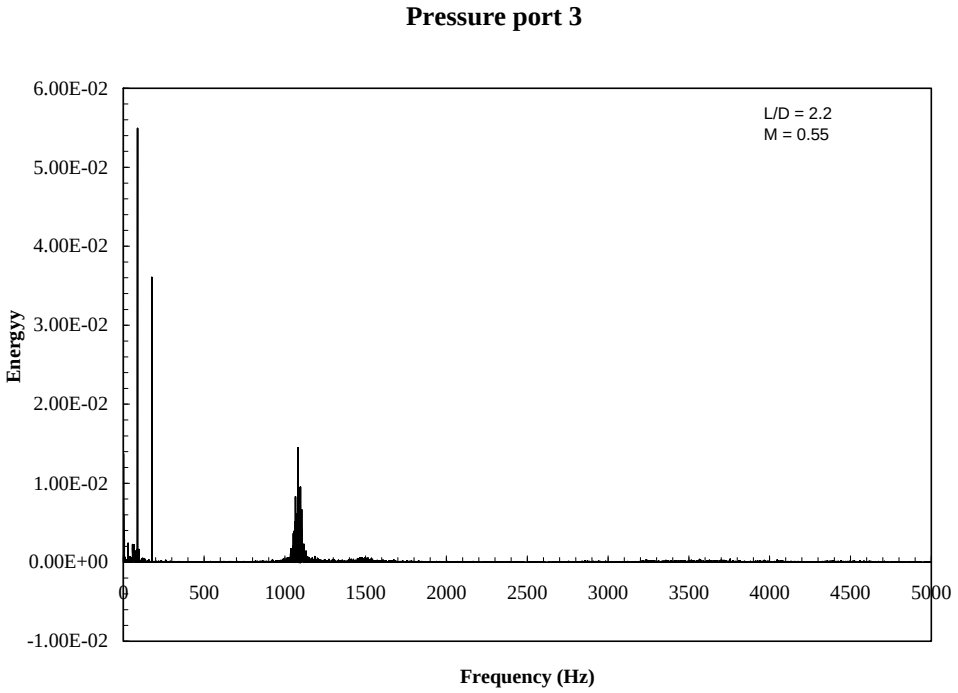


Figures 13 a), b), c) Spectra from kulites at ports 1, 2, and 3 respectively, M=0.55, L/D=4.0 with an aft cover length equal to 0.45 of L.

**Pressure port 1**

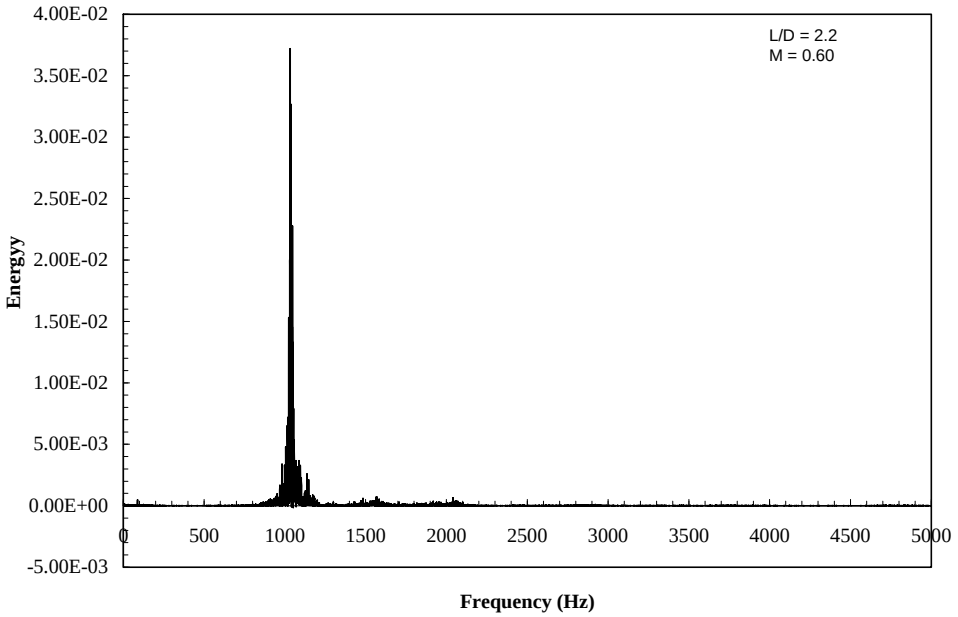


**Pressure port 2**

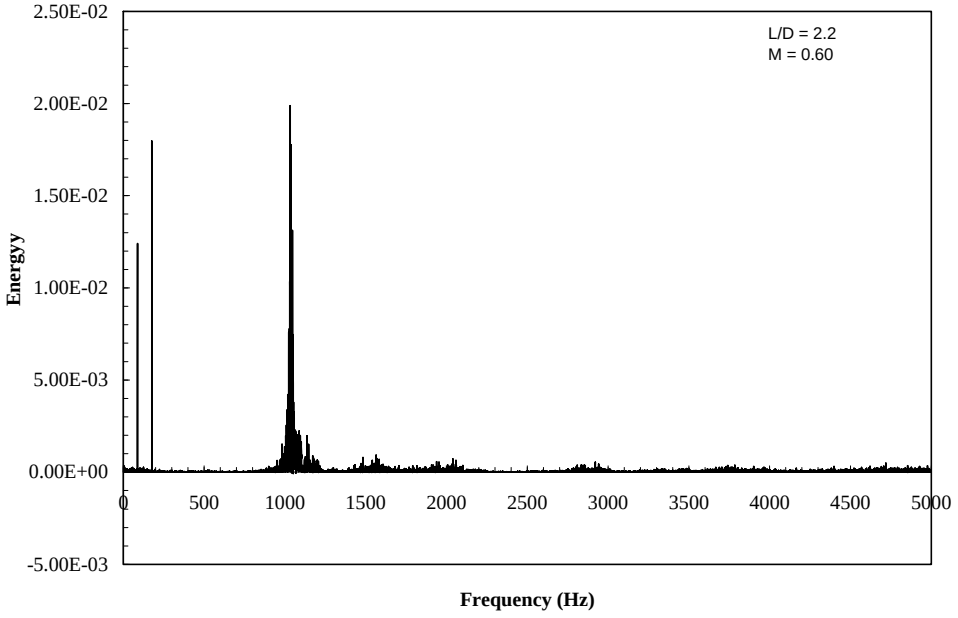

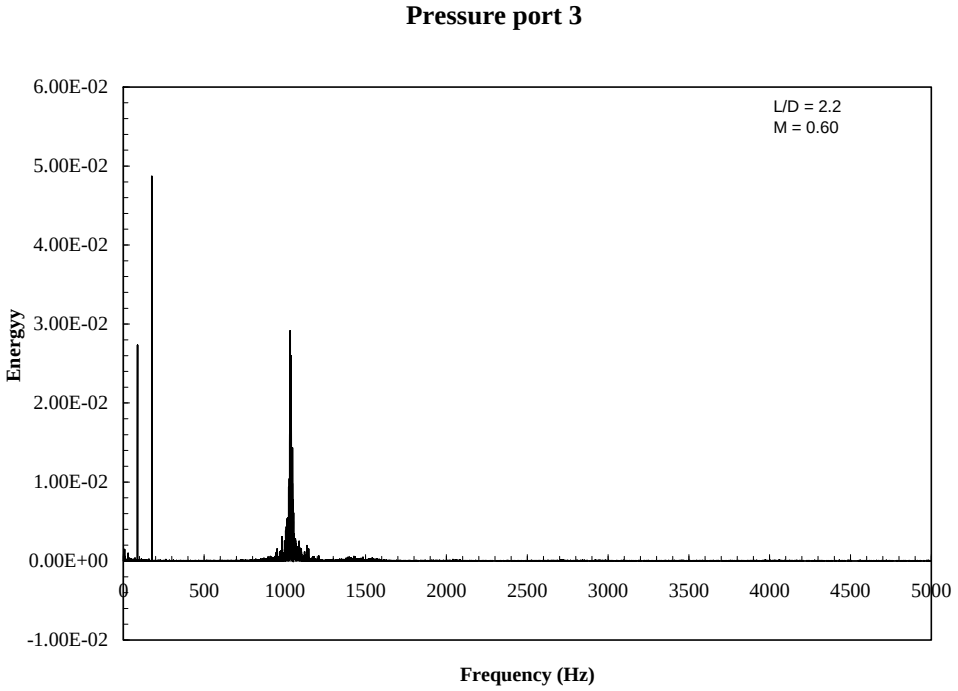


Figures 14 a), b), c) Spectra from kulites at ports 1, 2, and 3 respectively, M=0.60, L/D=4.0 with an aft cover length equal to 0.45 of L.

**Pressure port 1**

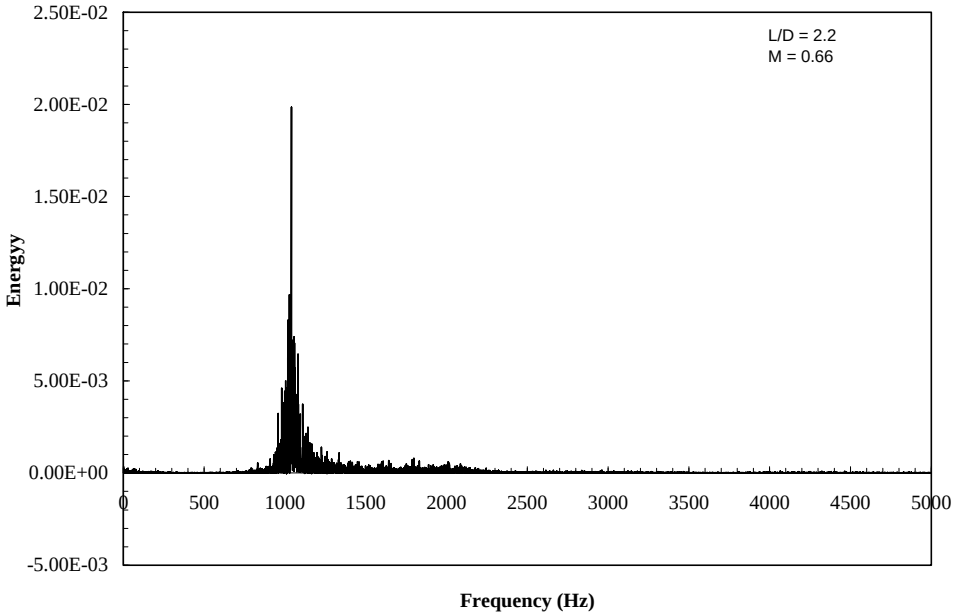


**Pressure port 2**

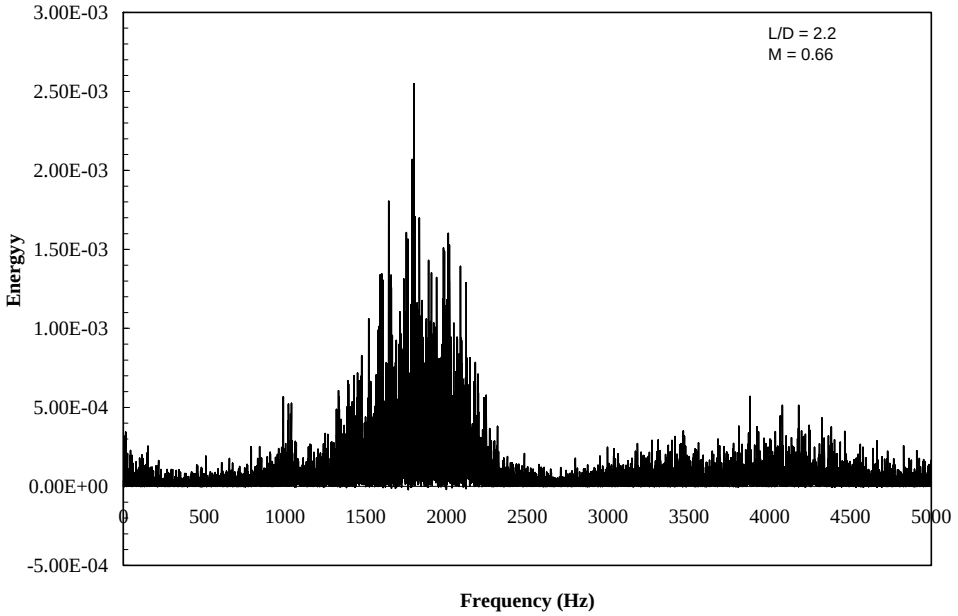

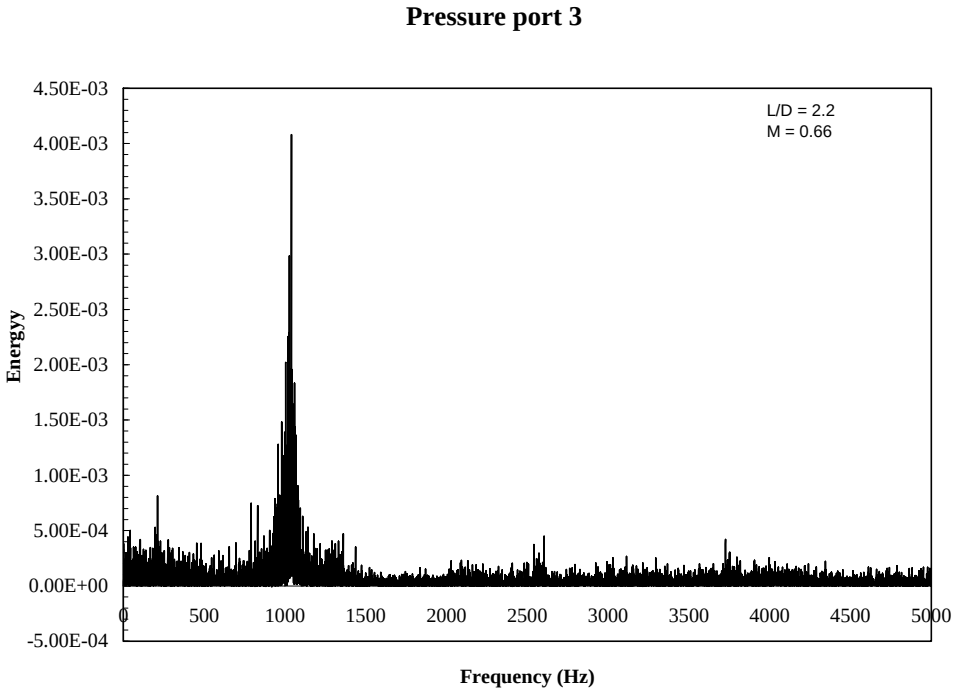


Figures 15 a), b), c) Spectra from kulites at ports 1, 2, and 3 respectively, M=0.66, L/D=4.0 with an aft cover length equal to 0.45 of L.

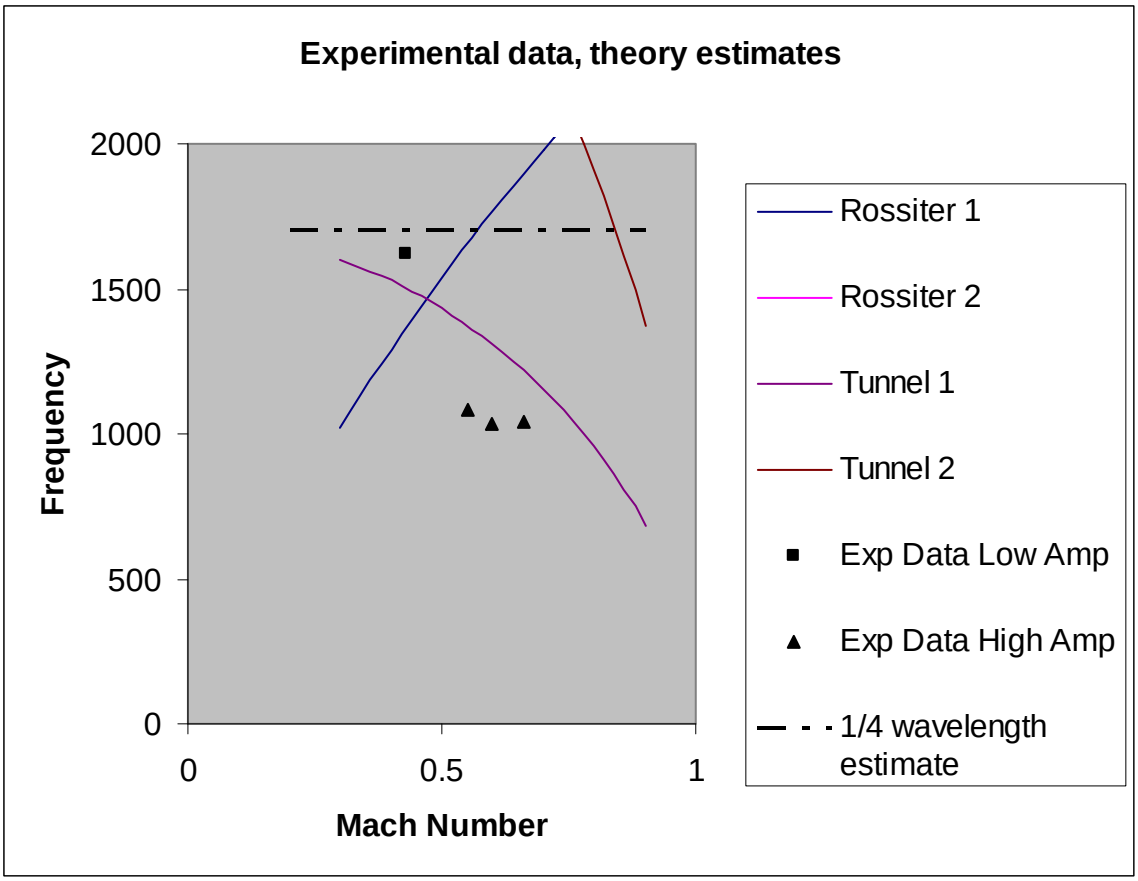


Figure 16 Experimental data and theory estimates for the small turret with an aft fairing studies with L/D=2.17 (see Figures 8 and 9).

Small Model L/D=2.17 case

| Mach | Freq | Amp |
|---|---|---|
| 0.43 | 1619 | 0.00842 |
| 0.55 | 1082 | 0.0324 |
| 0.6 | 1033.5 | 0.037195 |
| 0.66 | 1040 | 0.019834 |
| 0.2 | 1704 | |
| 0.9 | 1704 | |

Table 5 Frequency and amplitude data for L/D=2.17

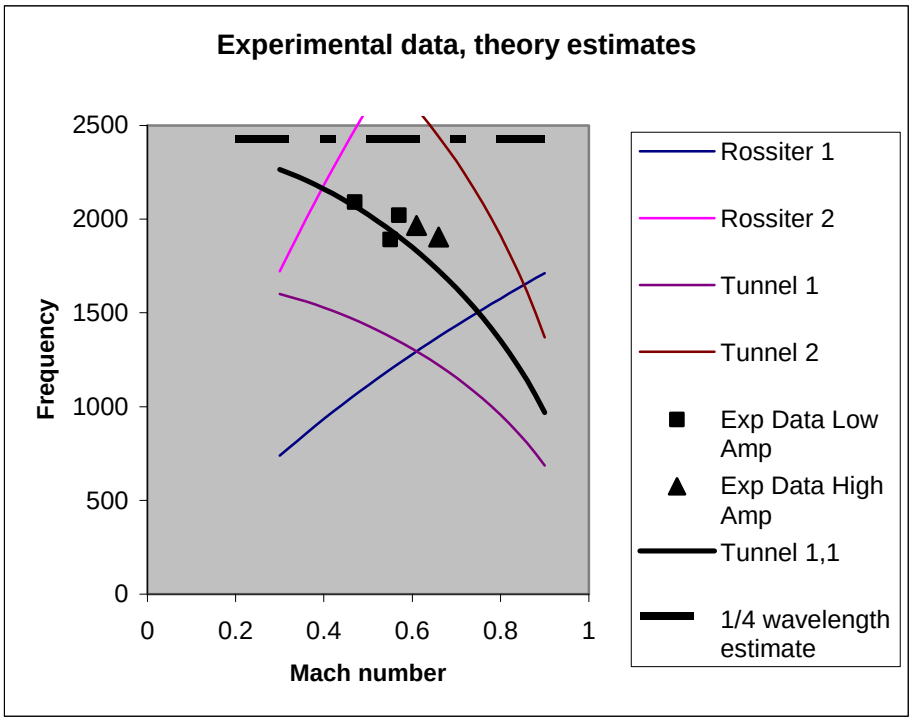


Figure 17 Experimental data and theory estimates for the small turret with an aft fairing studies with L/D=3.0

Small model L/D=3.0 case

| Mach | Freq | Amp |
|---|---|---|
| 0.47 | 2090.5 | 0.004354 |
| 0.55 | 1891 | 0.007748 |
| 0.57 | 2020 | 0.007225 |
| 0.61 | 1966 | 0.039556 |
| 0.66 | 1905 | 0.045486 |
| 0.2 | 2426 | |
| 0.9 | 2426 | |

Table 6 Frequency and amplitude data for L/D=3.0

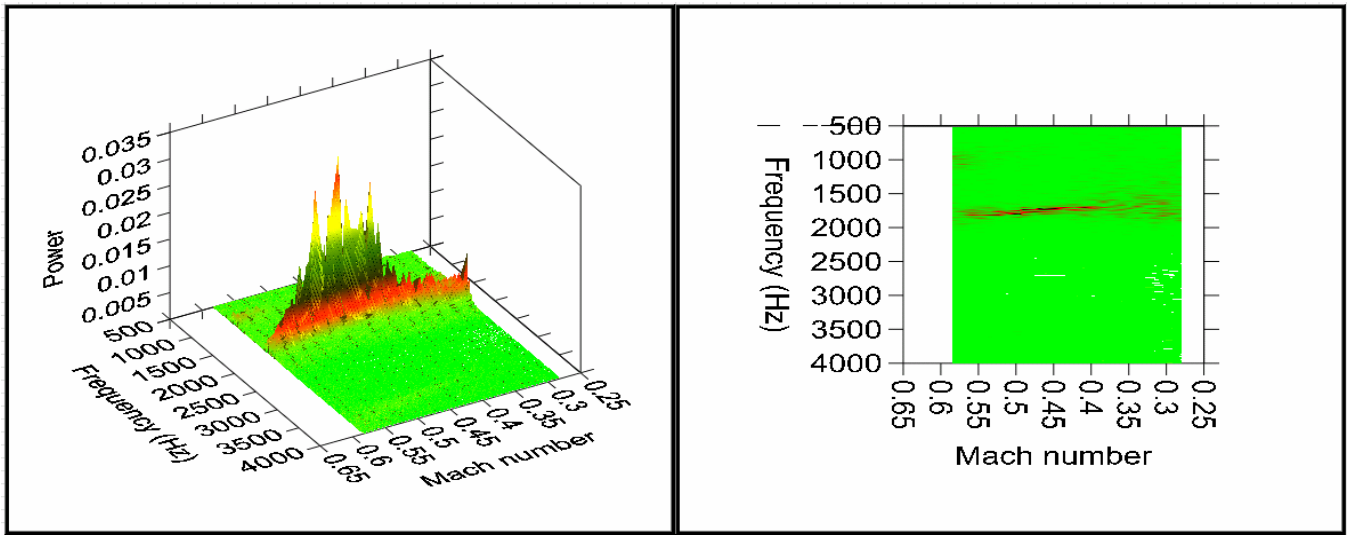


Figure 18 Kulite measured unsteady pressure data taken over a range of Mach numbers for a small patent pending model design

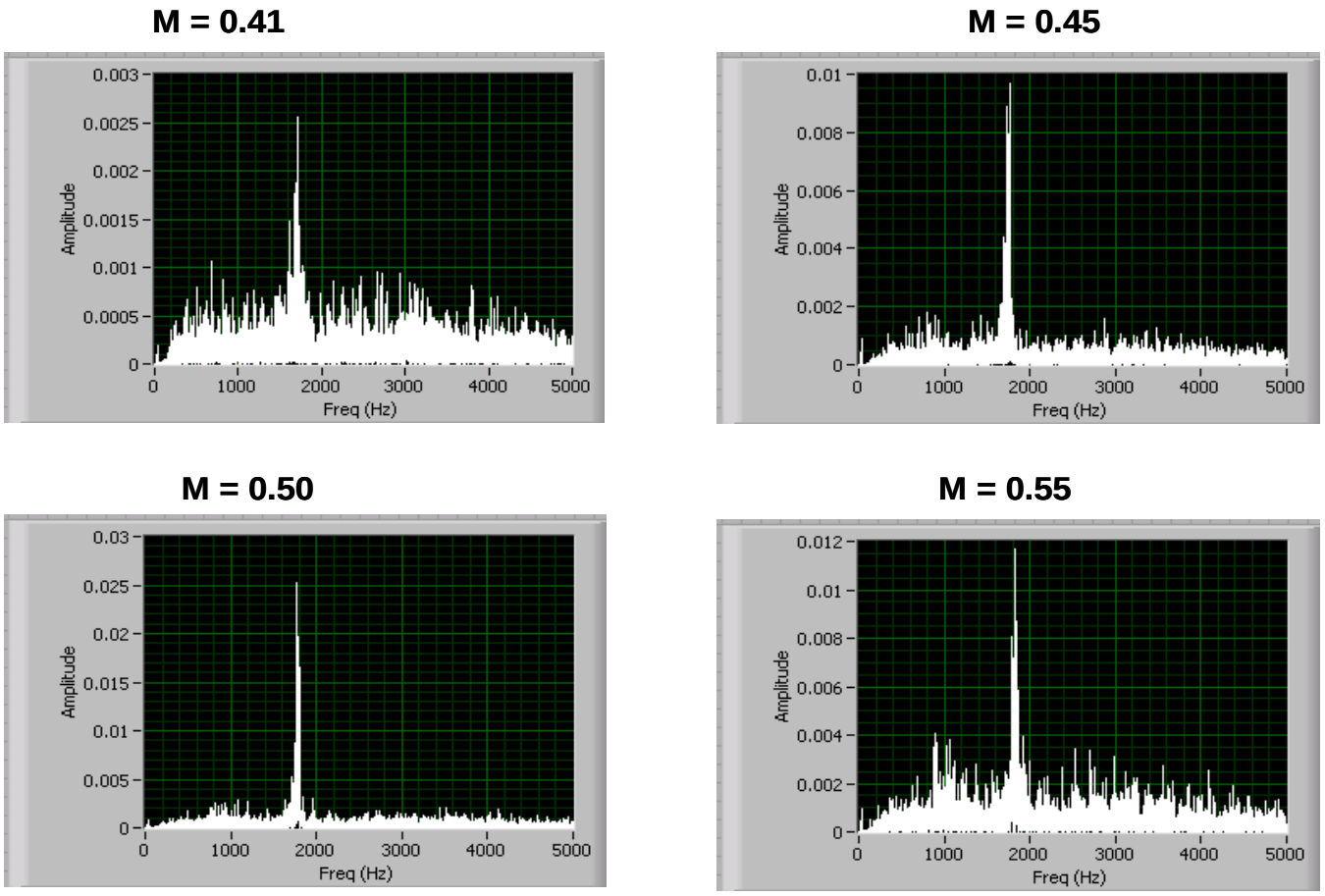


Figure 19 Optically measured spectral data taken at selected Mach numbers for a small patent pending model design